Interactions of Polyvinylpyrrolidone with Chlorin e6-Based Photosensitizers Studied by NMR and Electronic Absorption Spectroscopy

ARTICLE *in* THE JOURNAL OF PHYSICAL CHEMISTRY B · AUGUST 2015

Impact Factor: 3.3 · DOI: 10.1021/acs.jpcb.5b05761 · Source: PubMed

4 AUTHORS, INCLUDING:

Ilche Gjuroski

Universität Bern

3 PUBLICATIONS **7** CITATIONS

SEE PROFILE

Julien Furrer

Universität Bern

81 PUBLICATIONS **1,119** CITATIONS

SEE PROFILE

Martina Vermathen

Universität Bern

22 PUBLICATIONS **512** CITATIONS

SEE PROFILE

THE JOURNAL OF PHYSICAL CHEMISTRY B

Article

pubs.acs.org/JPCB

Interactions of Polyvinylpyrrolidone with Chlorin e6-Based Photosensitizers Studied by NMR and Electronic Absorption Spectroscopy

Marianne Hädener,[†] Ilche Gjuroski, Julien Furrer, and Martina Vermathen*

Department of Chemistry and Biochemistry, University of Bern, Freiestrasse 3, CH-3012 Bern, Switzerland

Supporting Information

ABSTRACT: Polyvinylpyrrolidone (PVP) can act as potential drug delivery vehicle for porphyrin-based photosensitizers in photodynamic therapy (PDT) to enhance their stability and prevent porphyrin self-association. In the present study the interactions of PVP (MW 10 kDa) were probed with five different derivatives of chlorin e6 (CE6) bearing either one of the amino acids serine, lysine, tyrosine or arginine, or monoamino-hexanoic acid as substituent. All derivatives of CE6 (xCE) formed aggregates of a similar structure in aqueous buffer in the millimolar range. In the presence of PVP monomerization of all xCE aggregates could be proved by ^{1}H NMR spectroscopy. xCE-PVP complex formation was confirmed by ^{1}H NMR T_2 relaxation and diffusion ordered spectroscopy (DOSY). ^{1}H^{1}H-NOESY data suggested that the xCE uptake into the PVP polymer matrix is governed by hydrophobic interactions. UV−vis absorption and fluorescence emission bands of xCE in the micromolar range revealed characteristic PVP-induced bathochromic shifts. The presented data point out the potential of PVP as carrier system for amphiphilic derivatives of chlorin e6. The capacity of PVP to monomerize xCE aggregates may enhance their efficiency as possible photosensitizers in PDT.

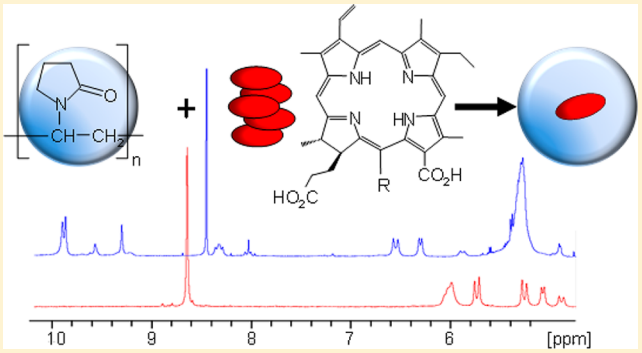

INTRODUCTION

Over the past decades, porphyrinic compounds have gained increasing interest as photosensitizers in photodynamic therapy (PDT) and diagnosis (PDD) of both, cancerous and noncancerous diseases. PDT is based on the selective destruction of a target tissue, e.g., tumors, by light irradiation of the photosensitizer enriched tissue. Photosensitizers usually exhibit a low dark toxicity but are able to create highly cytotoxic singlet oxygen and related reactive oxygen species (ROS) upon light excitation in the presence of oxygen. On the basis of this multifactorial combination of photosensitizer, light and oxygen, PDT has become a very promising alternative treatment modality of cancer with enhanced selectivity and reduced side effects as compared to conventional methods.[1,2]

The development of porphyrinic compounds with improved properties for their use as photosensitizing drugs has been guided by several aspects, such as (i) shifting the light absorption maximum to longer wavelengths (600−800 nm) where light exhibits better tissue penetration, (ii) enhancing the water solubility, (iii) improving the stability, (iv) enhancing the affinity for proliferative tissue, or (v) increasing the singlet oxygen quantum yield.[3]

Among the porphyrinic compounds, chlorins, which are dihydroporphyrins, have become of particular interest because they exhibit a strong light absorption in the range between 600−700 nm. Moreover, derivatives of chlorin e6 have amphiphilic structures so that their hydrophilicity−lipophilicity balance provides the potential both, for being transported in the bloodstream on one hand, and for sufficient membrane penetration in the tumor tissue on the other hand.[4] In particular amino acid derivatives of chlorin e6 have been suggested to be efficient photosensitizer drug candidates,[5−7] and mono-L-aspartyl chlorin e6 (talaporfin sodium, NPe6) has been approved in Japan about ten years ago for the treatment of lung cancer.[8] Besides improved water solubility amino acid moieties have been shown to enhance the interactions with cell membranes and yield porphyrin conjugates with highly efficient photosensitizing properties.[7,9−11]

Preventing porphyrin self-association is one of the aims in the development of the so-called third generation photosensitizers, which focuses on the use of drug delivery systems for porphyrinic compounds.[3,12,13] Indeed, even the amino acid derivatives of chlorin e6 despite their water solubility exhibit aggregation in aqueous media to different extents.[14]

Among the various systems, polyvinylpyrrolidone (PVP) has been successfully applied as carrier for chlorin e6 (CE6) and a CE6-PVP formulation called Photolon has been approved for PDT and PDD.[15] Complexes of CE6 and PVP have been

Received: June 16, 2015
Revised: August 14, 2015
Published: August 20, 2015

DOI: 10.1021/acs.jpcb.5b05761
J. Phys. Chem. B 2015, 119, 12117−12128

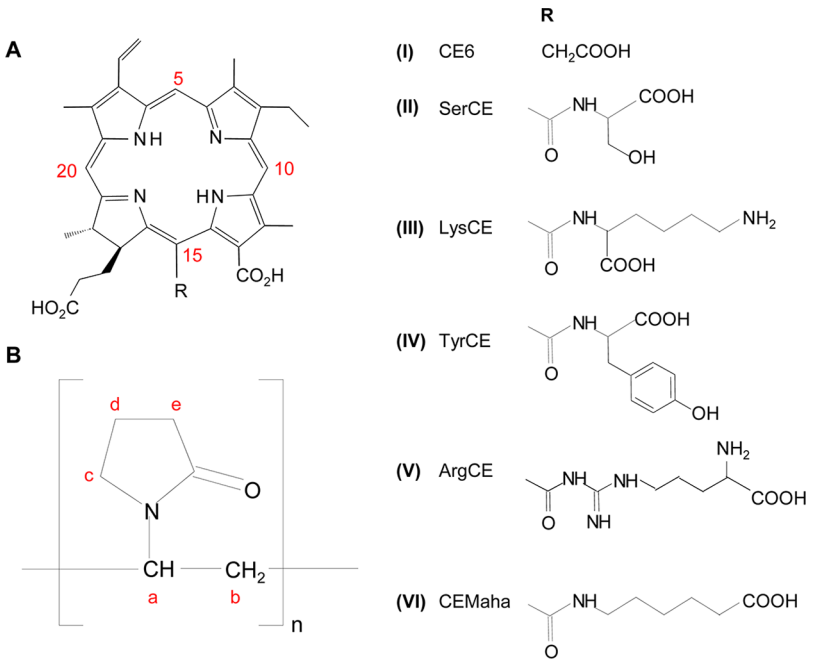

Figure 1. Structures of (A) chlorin e6 derivatives and (B) PVP.

extensively studied with respect to their biodistribution and pharmacokinetics,[16−18] their intracellular localization,[19] interactions with lipoproteins,[20] and possible cell death mechanisms.[15,19] It could be shown that PVP has the capacity to monomerize CE6 aggregates.[21,22]

The aim of the current study was to probe the capacity of PVP for monomerization of a series of five different amino acid derivatives of CE6, shown in Figure 1. ^{1}H NMR spectroscopy was used as main tool complemented by UV−vis and fluorescence spectroscopic methods to assess complex formation and intermolecular interactions. As a new approach for studying chlorin−PVP systems, specific ^{1}H NMR techniques including T_2 relaxation time measurements, diffusion and ^{1}H^{1}H-NOESY experiments have been applied to gain more detailed information on the dynamic behavior and interactions on a submolecular level.

EXPERIMENTAL SECTION

Materials. The porphyrinic compounds chlorin e6 (CE6, I), chlorin e6 serine amide trisodium salt (SerCE, II), chlorin e6 monolysine amide trisodium salt (LysCE, III), monotyrosine amide of chlorin e6 trisodium salt (TyrCE, IV), arginine amide of chlorin e6 trisodium salt (ArgCE, V), and chlorin e6 mono-6-amino-hexanoic acid amide (CEMaha, VI) were purchased from Frontier Scientific. The structures of the chlorin derivatives xCE (I − VI) are shown in Figure 1A. Polyvinylpyrrolidone (PVP, average MW 10 000) was purchased from Sigma-Aldrich. The PVP structure is shown in Figure 1B. The deuterated solvents D_2O (D 99.9%) and DMSO-d_6 were obtained from Cambridge Isotopes Laboratories, Inc. All chemicals and solvents were used without further purification. Phosphate buffered saline (PBS) solution of neutral pH (pH = 7) was prepared by mixing aliquots of 10 mM or 50 mM solutions of KH_2PO_4 and Na_2HPO_4 (both Sigma-Aldrich) in D_2O or H_2O containing 0.9% NaCl.

Nuclear Magnetic Resonance (NMR) Spectroscopy. The NMR experiments were performed on a Bruker Avance II spectrometer operating at a resonance frequency of 400.13 and 100.62 MHz for ^{1}H- and ^{13}C-nuclei, respectively. The instrument is equipped with a 5 mm dual broadband probe ("Bruker-*Smartprobe*") for direct detection with a z-gradient coil. If not otherwise mentioned, all 1D and 2D NMR measurements were carried out slightly above room temperature at 303 K to ensure a stable temperature.

1D ^{1}H NMR Spectroscopy. The ^{1}H NMR spectra were recorded using a 1D NOESY presaturation sequence with spoil gradients for residual water suppression ("*noesygppr1d*" from the Bruker pulse-program library). Typically, 64 transients were acquired over a spectral width of 12 ppm, with a data size of 64 K points, a noesy mixing time of 20 ms, and a relaxation delay of 6 s.

Acquisition and processing of all NMR spectra were performed using the Bruker Topspin software (version 2.1 and 3.0). Processing included for all 1D NMR spectra Fourier transformation of the coadded free induction decays (FIDs) after exponential multiplication with a line broadening factor of 1.0 Hz, as well as phase and baseline correction using a fifth order polynomial.

Spectral ^{1}H-resonance assignments were based on previously published data[14] and on additional standard 2D homo- and heteronuclear methods including 2D ^{1}H^{1}H−COSY, ^{1}H^{13}C-HSQC, ^{1}H^{13}C-HMBC, and ^{1}H^{1}H-ROESY experiments ("*cosygpqf*", "*hsqcedetgpsisp*", "*hmbcetgpl3nd*", and "*roesyphpr*", from the Bruker pulse-program library).

Temperature Dependence of ^{1}H NMR Spectra. The temperature dependence of ^{1}H NMR chemical shifts for 1.8 mM solutions of SerCE and LysCE in D_2O−PBS were determined as previously described for the related CE6 derivatives **I** and **IV**−**VI**.[14] The chemical shifts of the single xCE proton resonances (Figures S1 and S2) were then plotted as a function of temperature and linear regressions yielded the slope $a(Hx)$ for each of the proton resonances (Figures S3 A and S4 A). The difference in temperature dependence $\Delta(a(Hx))$ of chemical shifts with respect to the DMSO resonance shift (average slope $a(-CH_3)$DMSO = 0.101) were plotted as bars for SerCE and LysCE protons (Figures S3 B and

DOI: 10.1021/acs.jpcb.5b05761
J. Phys. Chem. B 2015, 119, 12117−12128

S4 B). These bar plots point out those protons, which exhibit largest temperature dependence and thus participation in aggregate formation. Linear regression of chemical shifts was performed with Microsoft Excel, version 2010.

NMR Transverse Relaxation Times T_2 of SerCE. Transverse relaxation times T_2 of 3 mM SerCE/PBS, 10 mM PVP/PBS, and SerCE-PVP (3:10)/PBS were measured applying the Carr−Purcell−Meiboom−Gill sequence (*"cpmg"* from the Bruker pulse-program library). For this, a randomly ordered series of 14 spectra with a 90° pulse of 12.6 μs, an interpulse delay of 0.5 ms with echo times ranging from 8 to 420 ms, a relaxation delay of 4 s and 16 scans per spectrum was acquired at a temperature of 303 K. T_2 relaxation times of the individual SerCE and PVP resonances were obtained from exponential fitting of peak integrals (SerCE) or peak intensities (PVP) using the Bruker Topspin software.

NMR Titration of xCE Stock Solution with PVP. xCE/PVP mixtures in D_2O-based PBS (50 mM) were prepared with a fixed xCE concentration of 3 mM and PVP concentrations varying from 1 to 20 mM. For this, aliquots of PVP stock solutions (13 mM or 25 mM) were diluted with an appropriate amount of PBS and stirred at room temperature. After ∼10 min, xCE stock solution was added to yield the desired xCE/PVP molar ratios. The resulting solution was stirred for ∼10 min and after an additional 10 min of equilibration 1D ^{1}H NMR spectra were recorded. For comparison, ^{1}H NMR spectra of pure 3 mM xCE and pure PVP solutions were acquired. Furthermore, 1D ^{1}H NMR spectra of 3 mM chlorin solutions in DMSO-d_6 were recorded. To visualize the magnitude of induced changes on the ^{1}H NMR chemical shifts δ of the single chlorin resonances in pure PBS δ_0 (xCE) and in the presence of 20 mM PVP δ_{PVP} (xCE), the differences $\Delta\delta$ (xCE) were calculated according to

$$\Delta\delta(\mathrm{xCE}) = \delta_{PVP}(\mathrm{xCE}) - \delta_0(\mathrm{xCE}) \tag{1}$$

and plotted as bars for each resonance.

To analyze the uptake curves the ^{1}H NMR chemical shift differences $\Delta\delta$ of the chlorin resonances in the aromatic region were plotted as a function of PVP concentration. Data points were fitted using the rectangular hyperbola function[23,24]

$$\Delta\delta = \Delta\delta_{\max} \times \frac{a[PVP]}{1 + a[PVP]} \tag{2}$$

with the Origin software (version 9.1, 2015 G, OriginLab Corporation). The resulting fit parameters are given in Table S1.

Determination of Intermolecular Distance by 2D Nuclear Overhauser Enhancement Spectroscopy (NOESY). To determine intermolecular distances between xCE and PVP, 2D NOESY spectra (*"noesygpphpr"*, modified Bruker pulse-program) were recorded for xCE/PVP 3:20 molar mixtures. The 2D NOESY were acquired with 2048 data points in F2, 512 in F1, with 64 scans per increment over a spectral width of 4800 Hz and an acquisition time of 0.21 s. NOE mixing time was set to 100 ms and relaxation delay to 1 s. Interproton distances were calculated by assuming that the ratio of the volumes of a pair of NOE cross peaks is proportional to the ratio of their internuclear distances:[25]

$$\frac{\eta_{I1}}{\eta_{I2}} = \frac{r_2^{\,6}}{r_1^{\,6}} \tag{3}$$

where r_1 is the known distance (1.78 Å) between the diastereotopic protons of the 15_1-CH_2 group,[25] η_{I1} is the volume of the corresponding NOE cross peak, r_2 is the unknown distance between two protons of interest and η_{I2} is the corresponding volume of the NOE cross peak. The intensities of the NOEs η_{I1} and η_{I2} were obtained by volume integration of the corresponding cross peaks in the 2D NOESY spectra. Volumes were corrected for the number of protons contributing to the cross peak.

NMR Diffusion Ordered Spectroscopy (DOSY) Measurements. To determine the diffusion coefficients, 2D ^{1}H diffusion ordered spectroscopy (DOSY) experiments were performed using a stimulated echo bipolar gradient pulse sequence with longitudinal eddy current delay and 2 spoil gradients (*"ledbpcpgp2sc"* or *"ledbpcpgp2scpr"* for water suppression from the Bruker pulse-program library). The gradient strength g_i was incremented in 16 steps along a linear ramp from 5 to 95% of its full strength of 55.45 G/cm using a sine-shaped gradient ("SINE.100", Bruker gradient shape library). The gradient length (δ) and the diffusion time (Δ) were optimized for each sample to achieve sufficient signal attenuation. Monoexponential fitting for selected resonances was applied to create the DOSY spectra using the Bruker software Dynamics Center 2.1.6.

Determination of the Dynamic Viscosity. Since the diffusion coefficient D is reciprocally proportional to the viscosity η according to the Stokes−Einstein equation

$$D = \frac{k_B T}{6\pi \cdot \eta \cdot r_s} \tag{4}$$

where k_B is the Boltzmann constant, T the temperature, and r_s the hydrodynamic radius of the solute, the viscosities of a 20 mM PVP solution in D_2O−PBS and of a pure D_2O−PBS solution were determined at 303 K with an Ostwald viscometer with a capillary of 5 mm diameter. The viscosities were determined to be 4.316 mPa s and 0.999 mPa s, for 20 mM PVP (in D_2O−PBS) and for pure D_2O−PBS, respectively. These values were used to calculate the theoretical D values of xCE in PBS with a hypothetical viscosity of a 20 mM PVP/PBS solution.

UV−Vis and Fluorescence Spectroscopy. The absorption spectra were recorded from 200 to 800 nm on a Varian Cary 100 Bio UV−visible spectrophotometer using a bandwidth of 2.0 nm and a scan rate of 600 nm/min. Fluorescence spectra were recorded from 410 to 800 nm on a Varian Cary Eclipse fluorescence spectrophotometer using the maximum of the Soret absorption band of the porphyrins as excitation wavelength (λ_{ex} = 399−402 nm) and a scan rate of 600 nm/min. The excitation and emission slits were set at a bandwidth of 5.0 nm. All measurements were carried out in quartz cuvettes (path length =10 mm) using 1 mL of sample volume and at 303 K. For the absorption and fluorescence measurements the xCE/PVP solutions used for NMR titration (s.a.) were diluted with 50 mM H_2O-based PBS to yield a final porphyrin concentration of 6 μM and PVP concentrations ranging from 2 to 40 μM. Pure H_2O−PBS solution served as blank. To analyze the uptake curves, the bathochromic shift of the absorption Q-band expressed as $\Delta\lambda$ [nm] was plotted as a function of PVP concentration. Data points were fitted using the rectangular hyperbola function[23,24]

DOI: 10.1021/acs.jpcb.5b05761
J. Phys. Chem. B 2015, 119, 12117−12128

$$\Delta\lambda = \Delta\lambda_{max} \times \frac{K_a[PVP]}{1 + K_a[PVP]} \quad (5)$$

with the Origin software (version 9.1, 2015 G, OriginLab Corporation). The resulting fit parameters are given in Table S2.

Cellular Uptake of SerCE-PVP. In order to confirm cellular uptake of PVP conjugates with the amino acid derivatives of CE6, cultured HeLa cells were incubated with SerCE in the absence and presence of PVP. As a control, cells were also incubated with PVP alone in the absence of SerCE. Cellular internalization following 2h incubation could be proved for SerCE-PVP by fluorescence microscopy. The obtained phase contrast and fluorescence images are shown in Figure S10. Experimental details are given in the Supporting Information.

RESULTS AND DISCUSSION

Five different derivatives of chlorin e6 (CE6), in which the acetyl side chain in position C-15 is conjugated either with the amino acids serine (SerCE, II), lysine (LysCE, III), tyrosine (TyrCE, IV), and arginine (ArgCE, V), or with monoaminohexanoic acid (CEMaha, VI) were investigated in this study (Figure 1A). For compounds I, IV, V, and VI, we have previously shown that they form aggregates in aqueous solution at neutral pH. Aggregation extent was most pronounced for ArgCE (V) and least for CE6 (I) and CEMaha (VI) while the aggregate structures appeared similar, i.e., the hydrophobic regions of the chlorin macrocyles overlapping.[14]

Aggregation Behavior of SerCE and LysCE. To probe the aggregation behavior of SerCE (II) and LysCE (III), temperature dependent ^{1}H NMR spectra were recorded of 1.8 mM solutions of each compound in aqueous buffer (PBS, pH 7, see Figures S1 and S2) as described previously.[14] In Figure 2

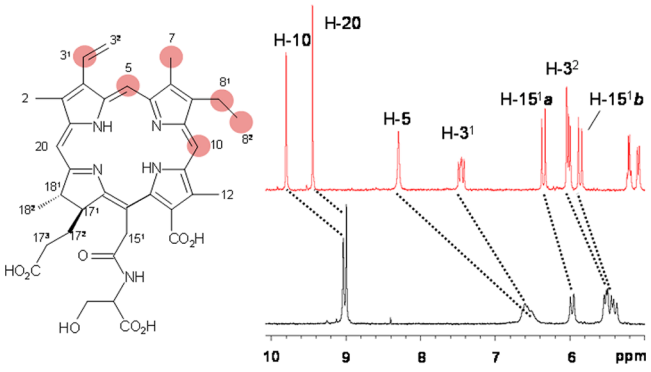

Figure 2. ^{1}H NMR spectra (aromatic region) of 1.8 mM SerCE in PBS at T = 298 K (black) and T = 343 K (red).

the aromatic regions of the ^{1}H NMR spectra of SerCE in PBS acquired at 298 K (bottom, black) and at 343 K (top, red) are shown together with the proton resonance assignment. The resonances of the three protons in meso-position H-5, H-10, and H-20 are upfield shifted and in part strongly broadened at room temperature, characteristic for aggregation (Figure 2). At 343 K, the ^{1}H-spectrum exhibits the typical downfield shift of the resonances and line narrowing, characteristic for disaggregation upon heating. The magnitude of this downfield shift is different for each proton and depends to a great extent on the ring current effect from neighboring porphyrin molecules and therefore on the orientation of the porphyrin ring. As such, aggregation maps obtained from plotting the chemical shift change as a function of the temperature for each single resonance (Figures S3 A and S4 A) indicate the protons which exhibit largest downfield shifts and thus areas of overlapping to form the aggregates (Figures S3 B and S4 B). These areas are indicated on the SerCE structure in Figure 2 and were found to be similar for LysCE (Figure S4 B). From these areas of overlapping, both amino acid derivatives SerCE and LysCE can be assigned to the same class of aggregate structures as was postulated for the remaining derivatives **I**, **IV**–**VI**.[14]

Interactions of Chlorin Derivatives (xCE) with PVP. The monomerization capacity of PVP for the chlorin derivatives **I**–**VI** (xCE) was investigated by mixing 3 mM xCE solutions in aqueous buffer with 10 mM PVP. In the absence of PVP, the ^{1}H NMR spectra (Figure 3, bottom

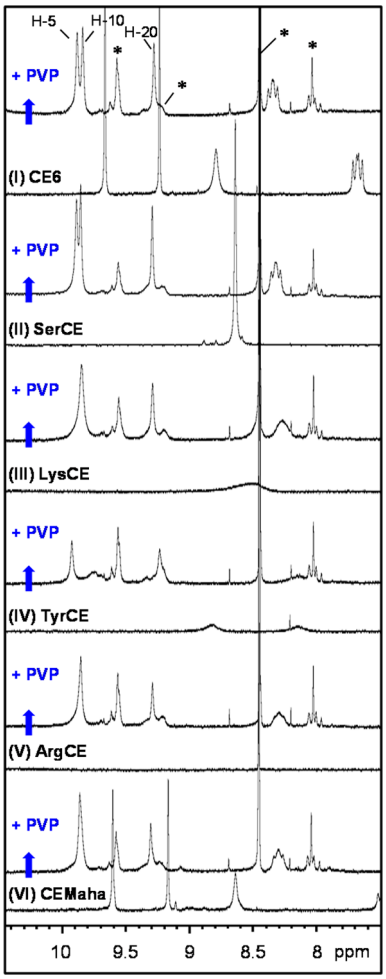

Figure 3. ^{1}H NMR spectra (aromatic region) of 3 mM chlorin derivatives in PBS (bottom spectrum) and after addition of 10 mM PVP (top spectrum) at T = 303 K. Peaks marked with ∗ are impurities from PVP.

spectra) indicated different degrees of aggregation. While ArgCE (V) did not give rise to any observable resonances in the aromatic region, very broad signals could be observed for TyrCE (IV) and LysCE (III), and only SerCE (II), CEMaha (VI) and CE6 (I) gave rise to sharp meso-proton resonances. Since NMR resonance line broadening caused by rapid transverse relaxation correlates with molecular size of the aggregates, it can be assumed that the aggregate size at neutral

DOI: 10.1021/acs.jpcb.5b05761
J. Phys. Chem. B 2015, 119, 12117–12128

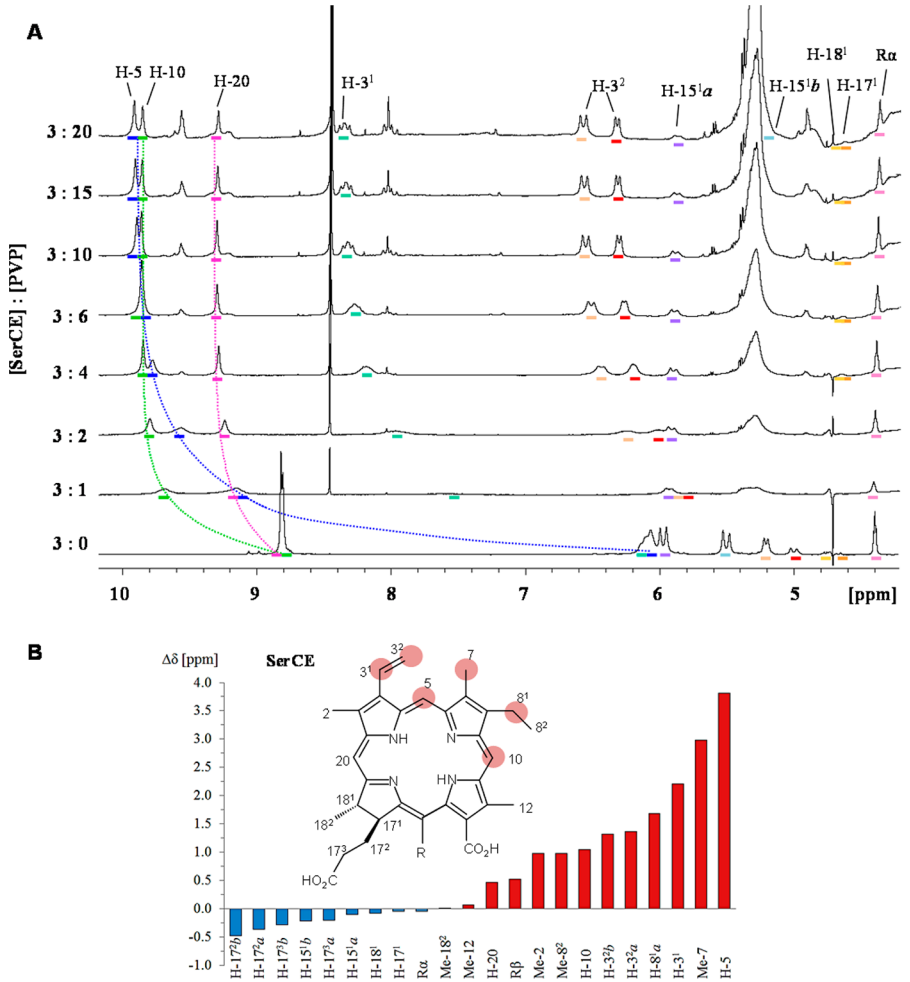

Figure 4. (A) ^{1}H NMR spectra (4−10 ppm region): titration of 3 mM SerCE with PVP in PBS; same resonances are indicated by same color. (B) Chemical shift difference $\Delta\delta$ for SerCE/PVP (3:20) compared to pure SerCE (3:0). Protons with $\Delta\delta > 1$ are highlighted in the structure.

pH follows the order ArgCE > LysCE ≈ TyrCE > SerCE ≈ CEMaha ≈ CE6. For all these derivatives bearing ionizable groups aggregation behavior is expected to be modulated by their pK_a values and the pH of the surrounding medium as has been shown for CE6.[26]

In the presence of 10 mM PVP, disaggregation could be observed for all xCE derivatives as clearly indicated by the appearance of the meso-proton resonances, pronounced downfield shifts and significant signal narrowing (Figure 3, top spectra). Most notably, the spectra of the different chlorin compounds exhibit very similar chemical shifts and line widths in the presence of PVP: The resonances of the meso-protons H-5 and H-10 overlap at around 9.85 ppm and the resonance of H-20 appears at 9.3 ppm. This similarity provides evidence that the corresponding chlorin protons have an equal microenvironment, namely the PVP network.

NMR Chemical Shift Titration of xCE with PVP. For quantitative evaluation of the interaction of chlorin derivatives with PVP, each compound was titrated with PVP increasing the concentration from 1 to 20 mM in aqueous buffer while keeping the xCE concentration constant at 3 mM. The corresponding spectra for the titration of SerCE are shown in Figure 4A for the spectral region between 4 and 10 ppm and the spectra for titrations of the remaining compounds **I** and **III**−**VI** are shown in Figures S5−S7.

The ^{1}H NMR spectra of SerCE undergo significant changes with increasing PVP concentration. These changes are most likely caused by two processes simultaneously taking place upon PVP titration: (i) dissolving of SerCE aggregates, and (ii) embedding of SerCE into the PVP polymer matrix. Besides an initial resonance broadening and subsequent gradual resonance narrowing, the single resonances of SerCE are strongly downfield (H-5, H-10, and H-20) or slightly upfield shifted (e.g., H-15 and H-17). The chemical shift differences with respect to pure SerCE in the absence of PVP ($\Delta\delta$) are shown in Figure 4B for a SerCE/PVP molar ratio of 3:20. Corresponding plots are shown for CE6, TyrCE and CEMaha in Figure S8. The most significant change was a downfield shift by about 4 ppm observed for the resonance of the meso-proton H-5 (Figure 4B). Notably, the regions of highest downfield shifts coincide with those marked in the aggregation map shown in Figure 2 suggesting that for these protons the main contribution derives from the PVP-mediated disaggregation of SerCE aggregates. Superimposed is a solvent-dependent shift of the resonances caused by the transition from the hydrophilic medium of the aqueous bulk phase toward a more hydrophobic one inside the polymer matrix. Likewise, the line widths of the chlorin resonances are affected by both processes, disaggregation leading to signal narrowing, and PVP complex formation leading to a slight signal broadening as can be seen for the proton resonances H-10 and H-20 of SerCE (Figure 4A). PVP

DOI: 10.1021/acs.jpcb.5b05761
J. Phys. Chem. B 2015, 119, 12117−12128

complex formation is confirmed by the transverse relaxation times T_2, which are inversely proportional to the resonance's line width (Table 1). While the T_2-values for the proton resonances of H-5 and H-3[1] increased upon addition of 10 mM PVP, those for the proton resonances H-10 and H-20 clearly decreased. The T_2 decrease is most likely a result of reduced molecular tumbling upon SerCE-PVP complex formation. Accordingly, the T_2-values slightly decreased for the PVP resonances H-c and H-d, reflecting the slightly larger size of the SerCE-PVP assembly compared to PVP alone. It should also be mentioned that a dynamic exchange process between the free (or self-assembled) and PVP-bound species of SerCE, which is intermediate or fast on the NMR time scale, takes place and also contributes to the observed line broadening effects. Thus, the SerCE resonances represent a weighted average of the two species increasingly shifting toward the PVP-bound form (Figure 4A). In accordance with these findings severe line broadening of chlorin meso-protons has been previously observed in an NMR study of a CE6-PVP system, which was performed at high CE6 excess (molar ratio CE6/PVP ~ 40:1).[27] Most likely this broadening was also due to a dynamic exchange process of the interacting components and seems to correspond to the first titration step of xCE shown here in Figure 4A and Figures S5–S7.

Table 1. Transverse Relaxation Time T_2 (± SD) of Selected SerCE and PVP Proton Resonances as Single Compounds in PBS and in a 3:10 Molar Mixture in PBS

		T_2 relaxation time [ms]		
		SerCE 3 mM	SerCE/PVP (3:10)	PVP 10 mM
SerCE	H-10	90.0 ± 6.0	54.5 ± 3.0	
	H-5	24.6 ± 1.3	42.8 ± 3.3	
	H-20	113.0 ± 7.8	71.3 ± 3.0	
	H-3[1]	24.6 ± 1.3	39.1 ± 2.6	
	H-3[2]*a*	40.1 ± 2.3	44.0 ± 3.7	
PVP	H-c		51.9 ± 3.1	57.5 ± 3.0
	H-d		78.4 ± 7.6	88.7 ± 8.7

PVP–Binding Curves. To compare PVP complex formation of the different chlorin derivatives **I–VI**, the chemical shift changes $\Delta\delta$ observed for the three meso-protons H-5, H-10, and H-20 were plotted as a function of PVP concentration, ranging from 0 to 20 mM (Figure 5). All chlorin derivatives **I–VI** yielded similar curves, the proton resonance H-5 exhibiting the largest and the proton resonances H-10 and H-20 exhibiting the smaller changes $\Delta\delta$, with the exception of LysCE, for which the chemical shift changes of H-10 and H-5 were similar. This may be due to a different orientation of H-10 within the dissolving aggregate whereas the final shift positions

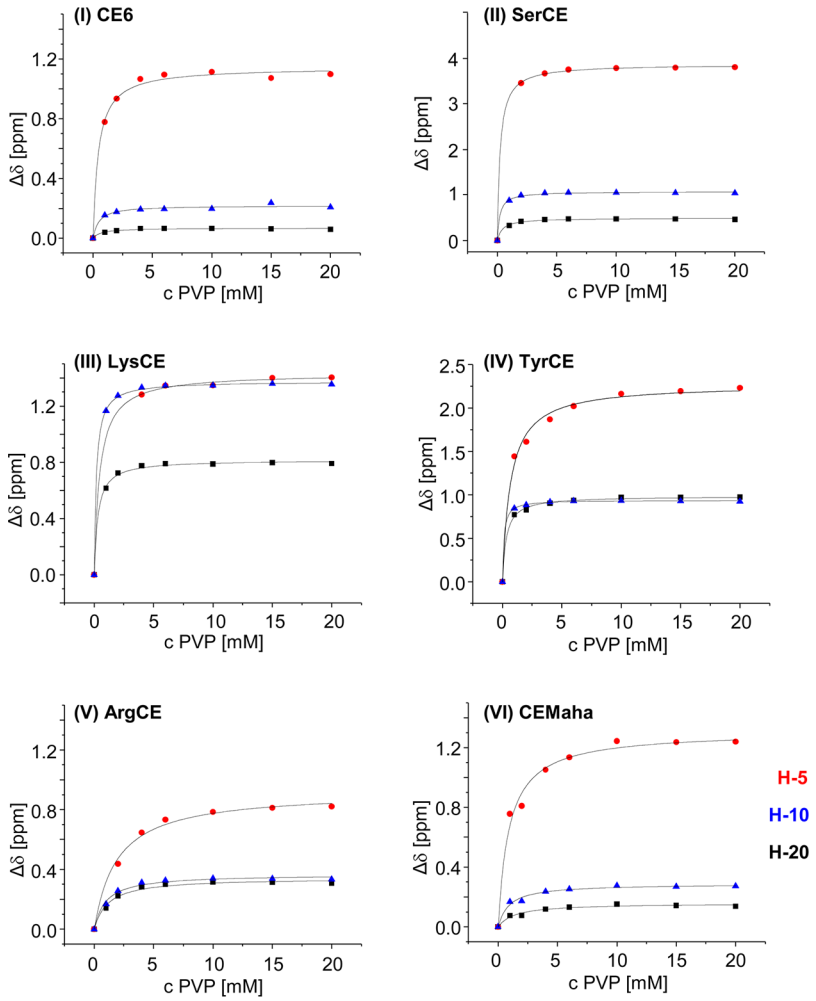

Figure 5. [1]H-chem. shift changes $\Delta\delta$ of chlorin meso-protons H-5 (red ●), H-10 (blue ▲), and H-20 (black ■) as a function of PVP concentration. Lines were obtained from nonlinear regression analysis.

DOI: 10.1021/acs.jpcb.5b05761
J. Phys. Chem. B 2015, 119, 12117–12128

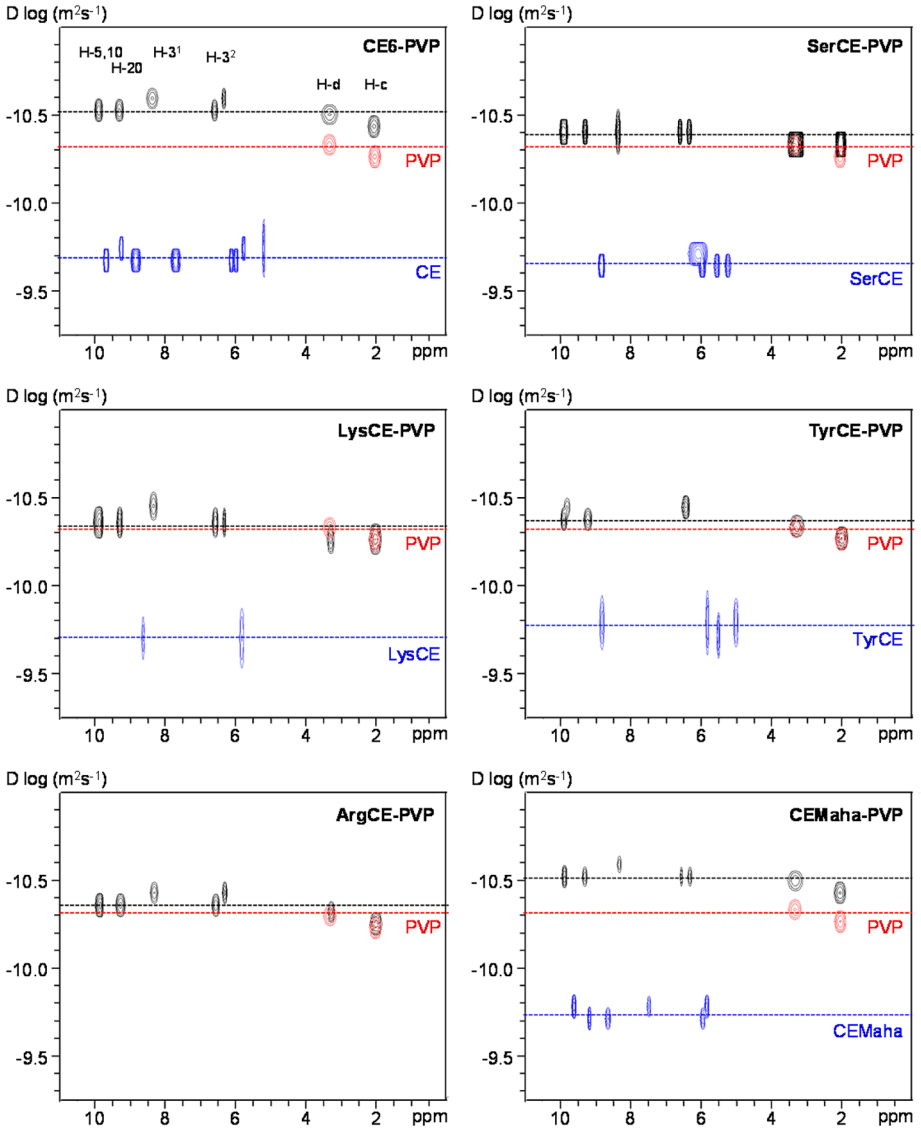

Figure 6. Overlay of 2D ^{1}H DOSY maps of the pure chlorin e6 derivative xCE (3 mM in PBS, blue), pure PVP (20 mM in PBS, red), and a mixture of xCE and PVP in PBS (molar ratio 3:20, black).

of the meso protons were all comparable among the xCE derivatives (Figure 3). The large shift changes $\Delta\delta$ observed for the proton resonances H-5 for all xCE derivatives ranging from 0.8 ppm (ArgCE) to almost 4 ppm (SerCE) seem to be mainly caused by PVP-induced disaggregation for all xCE derivatives.

Interestingly, all curves reach a plateau above a PVP concentration of ~5 mM suggesting that the formation of the xCE-PVP conjugate is approaching equilibrium. This corresponds to an average ratio xCE:PVP of 0.6, i.e. less than one xCE is bound per PVP. For the binding of CE6 with PVP the mean number of binding sites per PVP was estimated to be between 1.2 and 1.7 for PVPs of comparable molecular weights (8.2 and 11.7 kDa)[21] and 1.62 for PVP of the same molecular weight[22] as used in our study. These values were however obtained for a concentration in the micromolar range, where chlorin e6 is assumed to exist exclusively as monomers, whereas here, aggregation has to be taken into account. The steepest rise of $\Delta\delta$-values as a function of PVP concentration was observed for SerCE and LysCE while for ArgCE the curve increases more gently suggesting a higher affinity of SerCE and LysCE for PVP despite their different extents of aggregation (Figure 3). The binding affinity of small molecules to PVP-K30 (44−55 kDa) has been reported to correlate with hydrophobicity and log P values for a series of aromatic propionic acid derivatives.[28] As the polar distribution coefficients of serine and lysine lie between tyrosine and arginine[29,30] it seems likely that the affinity of the corresponding chlorin derivatives is guided by a combination of both, hydrophobicity and state of aggregation.

NMR Diffusion Ordered Spectroscopy (DOSY) of xCE-PVP Conjugates. ^{1}H NMR diffusion ordered spectroscopy (DOSY) is a powerful tool to monitor the formation of supramolecular complexes or host guest systems.[31] To provide evidence for xCE-PVP complex formation ^{1}H DOSY spectra were recorded for mixtures of the chlorin derivative (xCE) and PVP at molar ratios 3:20 as well as for equimolar solutions of either the pure chlorin compounds (3 mM) or pure PVP (20 mM) in PBS. The corresponding DOSY spectra are shown in Figure 6. In this Figure, each of the 2D-plots represents an overlay of 3 DOSY spectra measured for the mixture (shown in black) and for the single components (shown in blue for xCE and red for PVP, respectively). For ArgCE, the diffusion

DOI: 10.1021/acs.jpcb.5b05761
J. Phys. Chem. B 2015, 119, 12117−12128

Table 2. Diffusion Coefficients (±Error Estimated from Fit) of xCE and PVP as Pure Compounds in PBS and in Mixtures of xCE/PVP 3:20 Molar Ratio

	diffusion coefficient D [m^2 s^{-1}] × 10^{-11}				
	chlorin (3 mM)			PVP (20 mM)	
	PBS	PBSvisc[a]	PVP/xCE	PBS	PVP/xCE
PVP				4.32 ± 0.01	
(I) CE	16.9 ± 0.46	3.91	2.37 ± 0.04		2.91 ± 0.01
(II) SerCE	18.1 ± 0.27	4.19	3.36 ± 0.15		4.26 ± 0.05
(III) LysCE	17.2 ± 0.57	3.99	3.46 ± 0.20		4.26 ± 0.06
(IV) TyrCE	14.1 ± 2.8	3.27	3.32 ± 0.12		4.24 ± 0.04
(V) ArgCE	nd[b]	nd[b]	3.23 ± 0.26		4.10 ± 0.06
(VI) CEMaha	15.3 ± 0.34	3.54	2.43 ± 0.09		2.97 ± 0.03

[a]Calculated for a theoretical viscosity of 4.316 mPa s. [b]Not determined because of low signal-to-noise ratio.

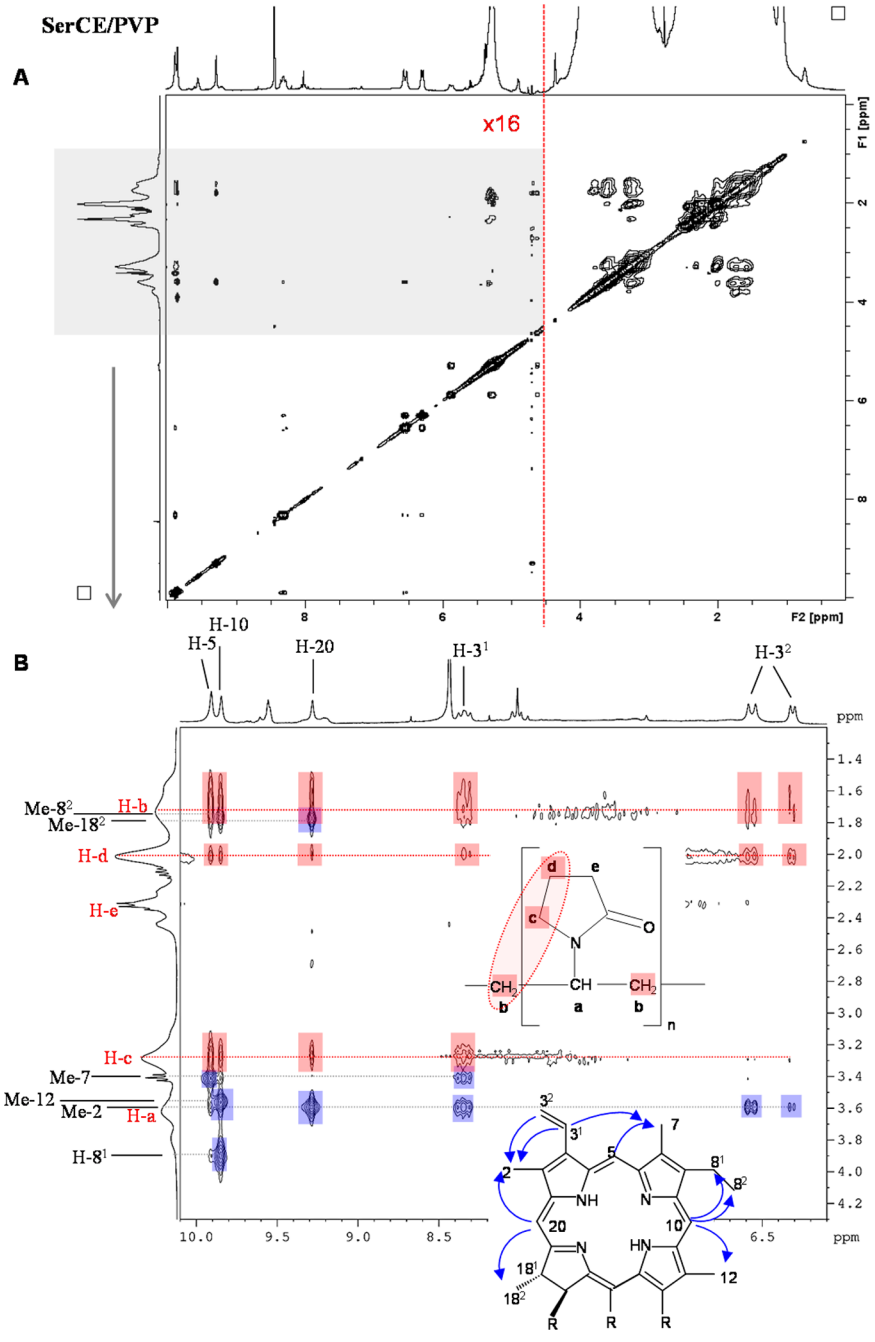

Figure 7. 2D $^1H^1H$-NOESY of SerCE/PVP (3:20) in PBS. (A) overview (B) expansion.

DOI: 10.1021/acs.jpcb.5b05761
J. Phys. Chem. B 2015, 119, 12117−12128

Table 3. Distances (±Estimated Error) between PVP Protons (H-b−H-e) and Porphyrin Meso-Protons (H-5, H-10, H-20) in xCE/PVP 3:20 Molar Mixtures

		interproton distance [Å]					
PVP	xCE	SerCE	CE6	LysCE	TyrCE	ArgCE	CEMaha
H-b	H-5	2.5 ± 0.38	2.2[a] ± 0.33	2.0[a] ± 0.3	2.3 ± 0.35	2.4[a] ± 0.36	2.3[a] ± 0.35
	H-10	2.8 ± 0.42			2.2 ± 0.33		
	H-20	2.8 ± 0.42	2.5 ± 0.38	2.4 ± 0.36		2.6 ± 0.39	2.5 ± 0.38
H-c	H-5	2.7 ± 0.41	2.3[a] ± 0.38	1.8[a] ± 0.27	2.4 ± 0.36	2.2[a] ± 0.33	2.2[a] ± 0.33
	H-10	3.0 ± 0.45			2.4 ± 0.36		
	H-20	3.1 ± 0.47	3.5 ± 0.35	3.5 ± 0.53	3.0 ± 0.45	3.1 ± 0.47	2.5 ± 0.38
H-d	H-5	3.3 ± 0.5	3.0[a] ± 0.45	2.0[a] ± 0.3		2.5 ± 0.38	2.3[a] ± 0.35
	H-10	3.4 ± 0.51				2.6 ± 0.39	
	H-20	3.8 ± 0.57		3.3 ± 0.5			2.4 ± 0.36
H-e	H-5						2.6[a] ± 0.39
	H-10						
	H-20						2.3 ± 0.35

[a]Average distance calculated due to overlap of meso-protons H-5 and H-10.

coefficient in the absence of PVP could not be determined in PBS because the signal-to-noise ratio was too low due to aggregation (see Figure 3). From the DOSY spectra it can be seen that in the presence of PVP the *D*-values of all chlorin derivatives I − VI are very similar to that of PVP, thus confirming complex formation. However, as diffusion coefficients are inversely correlated to the viscosity of the solution, the difference in viscosities in the absence and presence of 20 mM PVP has to be taken into account. Therefore, the *D*-values for xCE in the absence of PVP were calculated for a hypothetical PBS solution of the same viscosity as measured for 20 mM PVP. Table 2 summarizes the experimental and calculated *D*-values for each of the xCE compounds. Since 20 mM PVP increases the viscosity of a D_2O-based PBS solution by a factor of 4.3, it also has a large impact on the translated diffusion coefficients of the single chlorin compounds in PBS resulting in much smaller *D*-values. Nevertheless, the diffusion coefficients are still lower upon PVP-complex formation except for TyrCE (IV) (Table 2). This indicates the presence of large TyrCE aggregates in a similar molecular size range as the PVP polymers.

In the presence of compounds II − V, the diffusion coefficient of PVP ($4.1-4.26 \times 10^{-11}$ m^2 s^{-1}) was not significantly changed compared to PVP alone (4.32×10^{-11} m^2 s^{-1}) as is evident from the DOSY spectra (Figure 6) and the *D*-values given in Table 2. This is not surprising as in most host guest systems the contribution of the guest is negligible due to a large difference in molecular size.[32] Here, the average molecular weight ratio between PVP (MW ≈ 10 kDa) and xCE (MW ≈ 700) is approximately 14. However, in the presence of compounds **I** (CE6) and **VI** (CEMaha), the PVP resonances exhibit a noticeable reduction in their *D*-values as compared to pure PVP (Figure 6, Table 2). Similar to the NMR chemical shifts, the measured NMR diffusion coefficients likewise represent mole fraction weighted averages of the contributing components,[31,32] i.e., free PVP and PVP bound to xCE. Obviously, the amount of CE6 and CEMaha bound to PVP is higher than for the remaining xCE so that it has a clear effect on the diffusion rate of PVP in solution. For the same reason, the diffusion rates measured for the resonances of compounds **II**−**V** are slightly reduced as compared to the corresponding PVP resonances measured in the complex (Table 2). Since CE6 and CEMaha exhibited relatively sharp resonances in the absence of PVP (Figure S5 A and Figure 3) the amount of xCE incorporated into PVP at equilibrium may be controlled by the initial extent of aggregation.

2D $^1H^1H$-NOESY Spectra of xCE-PVP Conjugates. 2D $^1H^1H$-NOESY data were acquired to probe for intermolecular spatial proximity of protons and preferential sites of interaction between the chlorin and PVP components. The 2D NOESY spectrum obtained for a SerCE/PVP (3:20) mixture in PBS is shown in Figure 7. Notably, the sign of all NOE cross peaks was the same as the diagonal peaks, which is typical for large systems with long molecular correlation times.[33] Besides the intense intramolecular NOEs observed for the PVP protons (Figure 7A), informative weak NOEs between protons from the aromatic and aliphatic regions could be identified. Interesting *intermolecular* through-space interactions could be detected between the chlorin and PVP protons (highlighted in red in Figure 7B) supporting the 1D NMR and DOSY findings of chlorin-PVP complex formation. Similar 2D NOESY spectra were obtained for all xCE-PVP systems. To estimate the interproton distances, the cross peak volumes were calculated and calibrated against the NOE between the geminal protons of the 15_1-CH_2 group and their known distance of 1.78 Å.[25] The distances determined between the chlorin meso-protons and PVP protons are summarized in Table 3. Since there was a partial overlap of the H-5 and H-10 protons in some of the xCE spectra, average distance values were calculated in these cases for H-5 and H-10 intermolecular NOEs with PVP protons. Because of this overlap and the relatively low signal-to-noise ratio, the calculated interproton distances given in Table 3 are not precise but rather rough approximations. Nevertheless, comparing the NOEs within a given xCE-PVP system, distances to PVP protons were found to be shorter for the meso-proton H-5 or H-5/H-10, respectively, than for H-20. This suggests that substantial contribution in xCE-PVP complex formation derives from hydrophobic interactions with the less polar side of the amphiphilic chlorin macrocycle, which is also responsible for aggregate formation. Molecular dynamic simulation studies have proposed that PVP adopts a helical structure with the backbone protons (H-a and H-b) inside and pyrrolidone carbonyls exposed to the water.[34] As most intense NOEs were found between the meso-protons and the PVP protons H-b and H-c, these PVP protons seem to be the preferential binding sites for the hydrophobic interactions along with H-d as is highlighted in the PVP structure shown in Figure 7B. Hydrophobic interactions have also been reported as driving

DOI: 10.1021/acs.jpcb.5b05761
J. Phys. Chem. B 2015, 119, 12117−12128

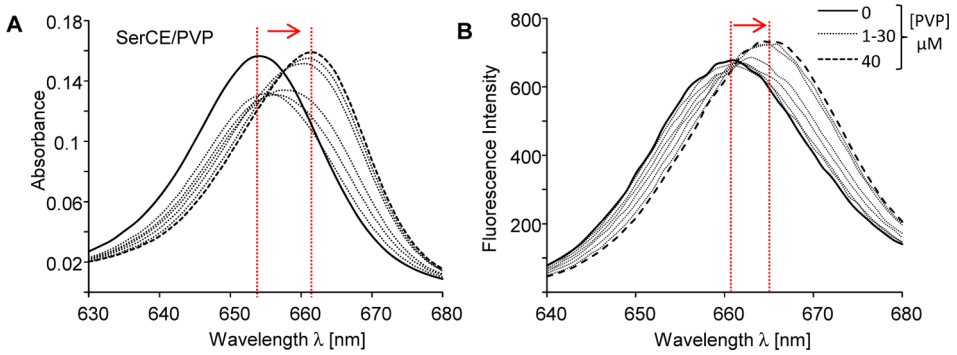

Figure 8. (A) Absorption spectra showing the Q-band and (B) fluorescence spectra (excitation: 400 nm) of SerCE (6 μM in PBS) as a function of PVP concentration.

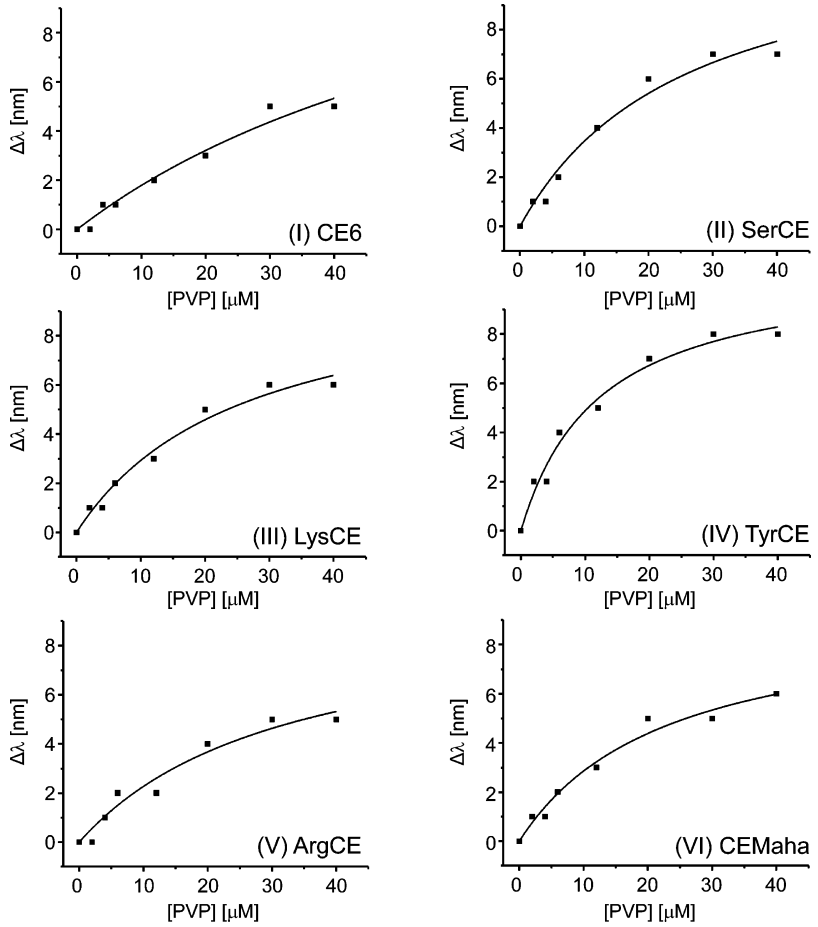

Figure 9. Q-absorption band shifts $\Delta\lambda$ of xCE as a function of PVP concentration. The chlorin concentration was kept constant at 6 μM. Lines correspond to nonlinear fitting.

force in CE6-PVP complex formation based on thermodynamic and molecular simulation data.[22,34] However, Zhiyentayev et al.[27] have postulated that both, hydrophobic and hydrophilic interactions contribute to CE6-PVP complex formation. This was concluded from an NMR study of a CE6-PVP system at excess CE6 analyzing the NMR signals of CE6 and PVP. In this paper, strongest changes were observed for the CE6 meso-protons and the PVP backbone protons (H-a and H-b), but all other proton resonances also exhibited line broadening and shifts including those of the PVP resonances assigned to the more hydrophilic pyrrolidone protons. The findings and conclusions were paralleled by previous results reported for a hematoporphyrin−PVP system.[35] In our study, the spectral changes of the PVP resonances, i.e., initial signal broadening and slight upfield shifts in the presence of xCE (Figure S9 for SerCE and LysCE) are similar as reported in these references. However, NOEs between the more polar xCE substituents and PVP could not be detected. Since these NOE cross peaks would be strongly overlapped and obscured by the intense intramolecular PVP cross peaks, hydrophilic contributions in complex formation cannot be ruled out, though. Nevertheless, CEMaha was the only chlorin derivative where the meso-protons gave rise to comparable NOEs with all PVP protons (except for H-a) suggesting a different PVP−complex structure

DOI: 10.1021/acs.jpcb.5b05761
J. Phys. Chem. B 2015, 119, 12117−12128

for this compound. The amino−hexanoic acid substituent in CEMaha most likely reduces its amphiphilicity, which may be responsible not just for the observed difference in PVP interaction but also for the comparably low extent of aggregation (see discussion of Figure 3).

Fluorescence and UV−Vis Absorption Spectra of Chlorin Derivatives xCE in the Presence of PVP. Previously, CE6-PVP interactions have been mainly studied by means of UV−vis-absorption or fluorescence spectroscopy.[21,22,27] As opposed to NMR spectroscopy, these studies are usually performed in the micromolar range, where the chlorin is assumed to exist as monomers.[21] Therefore, to compare the above NMR results, the xCE-PVP systems were submitted to absorption and fluorescence spectroscopy at a constant xCE concentration of 6 μM. Employing the same xCE/PVP molar ratios as for the NMR chemical shift titration, 6 μM solutions of xCE in PBS were titrated with PVP and their absorption and fluorescence emission spectra were monitored. Because of their partially hydrated porphyrin ring systems, chlorins exhibit an intense absorption band at around 650 nm. The absorption spectra displaying this Q-band in the course of SerCE titration with PVP are shown in Figure 8A. The corresponding fluorescence spectra monitoring the emission band of SerCE are displayed in Figure 8B. The changes in absorption band maxima $\Delta\lambda$ plotted as a function of PVP concentration are shown in Figure 9 for compounds **I**−**VI**. Similar curve progressions were obtained for all xCE derivatives. With increasing PVP concentration the Q-absorption band maximum exhibited a bathochromic shift by 5−8 nm. Likewise, the fluorescence emission maxima were shifted to longer wavelengths by an average of 4 nm (Table S3) while the fluorescence intensity was slightly increased (Figure 8B) upon PVP titration. Bathochromic shifts of both, absorption and fluorescence emission maxima have been reported for chlorin e6 upon PVP addition and were interpreted as CE6-PVP complex formation.[21,22,27] It could be ascribed to a solvatochromic effect caused by the change of the chlorin from the aqueous to the less polar PVP network environment.[21,27] Paul et al.[22] have attributed the shift to monomerization of CE6 aggregates upon PVP binding. However, they applied xCE concentrations higher by a factor of 12 as compared to our study. Therefore, it can be assumed that at the low xCE concentration applied in the present study, PVP binding seems to be the main contributor to the UV absorption and fluorescence emission shifts observed (Figure 9 and Table S3). In contrast, the NMR titration curves shown in Figure 5 were influenced by both, aggregation state and affinity for PVP, where SerCE and LysCE exhibited the most prominent progressions. The corresponding UV absorbance curves (Figure 9) however suggest that TyrCE has highest affinity for PVP, i.e. the xCE derivative with the least polar amino acid[29,30] of those probed in our study. This indicates that if aggregation is not a limiting factor, uptake and affinity for PVP are mainly governed by the hydrophobicity of the xCE side chains.

CONCLUSION

In the present study, the interaction of polyvinylpyrrolidone (PVP) with five different derivatives of chlorin e6 (xCE) bearing amino acids or amino-hexanoic acid has been probed for the suitability of PVP as xCE-carrier for its potential use in PDT. All xCE derivatives exhibited aggregation in neutral aqueous solution to different extents and showed similar aggregate structures. It could be shown, that PVP was capable to disaggregate all of the xCE derivatives, even the highest aggregated one (ArgCE). Both, monomerization of the chlorin and uptake into PVP could be proved by NMR spectroscopic chemical shift titration, T_2 relaxation, diffusion and 2D NOESY data. UV−vis and fluorescence spectroscopy applied to micromolar solutions of xCE-PVP systems confirmed the xCE uptake by PVP. According to the NMR data the binding of xCE to PVP seems to be controlled by a combination of hydrophobicity and initial extent of aggregation. While the DOSY data revealed higher uptake for the less aggregated species (CE6 and CEMaha), the 2D NOESY data indicated that xCE interactions with PVP were mainly governed by hydrophobic interactions with the less polar sites of the amphiphilic chlorin macrocycle. Likewise, in the absence of aggregates in the micromolar range, the UV−vis spectroscopic data suggest that the affinity for PVP uptake correlates with the hydrophobicity of the xCE side chain. In summary, PVP which has been successfully applied as carrier for chlorin e6, seems to be similarly well suited for amphiphilic derivatives of CE6. As aggregation and hydrophobicity are interdependent factors, PVP may be a most sufficient monomerizing carrier for xCE derivatives with "intermediate" properties such as SerCE and LysCE. Thus, PVP has the potential to improve the photosensitizing properties of several amino acid derivatives of CE6 and may promote their use as potent PDT drug candidates.

ASSOCIATED CONTENT

Supporting Information

The Supporting Information is available free of charge on the ACS Publications website at DOI: 10.1021/acs.jpcb.5b05761.

Additional ^{1}H NMR spectra and plots with linear regression as well as bar plots analyzing the chemical shift changes as a function of temperature or PVP concentration and additional fluorescence spectroscopy and microscopy data and fit parameters for the nonlinear regression analyses (PDF)

AUTHOR INFORMATION

Corresponding Author

*(M.V.) Telephone: +41 031 631 3948. Fax: +41 031 631 4887. E-mail: martina.vermathen@dcb.unibe.ch.

Present Address

†Institute of Forensic Medicine, University of Bern, Switzerland.

Notes

The authors declare no competing financial interest.

ACKNOWLEDGMENTS

We gratefully acknowledge the financial support obtained from the Swiss National Science Foundation (SNF), Grant No. 200021_149438.

ABBREVIATIONS

ArgCE, arginine amide of chlorin e6; CE6, chlorin e6; CEMaha, chlorin e6 mono-6-amino-hexanoic acid amide; Da, Dalton; DOSY, diffusion ordered spectroscopy; LysCE, lysine amide of chlorin e6; MW, molecular weight; NMR, nuclear magnetic resonance spectroscopy; NOE, nuclear Overhauser enhancement; NOESY, nuclear Overhauser enhancement spectroscopy;

DOI: 10.1021/acs.jpcb.5b05761
J. Phys. Chem. B 2015, 119, 12117−12128

PBS, phosphate buffered saline; PDD, Photodynamic diagnosis; PDT, photodynamic therapy; PVP, polyvinylpyrrolidone; SD, standard deviation; SerCE, serine amide of chlorin e6; TyrCE, tyrosine amide of chlorin e6; xCE, chlorin e6 derivative

REFERENCES

(1) Kiesslich, T.; Gollmer, A.; Maisch, T.; Berneburg, M.; Plaetzer, K. A Comprehensive Tutorial on In Vitro Characterization of New Photosensitizers for Photodynamic Antitumor Therapy and Photodynamic Inactivation of Microorganisms. *BioMed Res. Int.* **2013**, *2013*, 1−17.

(2) Benov, L. Photodynamic Therapy: Current Status and Future Directions. *Med. Prin. Pract.* **2015**, *24* (s1), 14−28.

(3) Lucky, S. S.; Soo, K. C.; Zhang, Y. Nanoparticles in Photodynamic Therapy. *Chem. Rev.* **2015**, *115* (4), 1990−2042.

(4) Uzdensky, A. B.; Dergacheva, O. Y.; Zhavoronkova, A. A.; Reshetnikov, A. V.; Ponomarev, G. V. Photodynamic Effect of Novel Chlorin e_6 Derivatives on a Single Nerve Cell. *Life Sci.* **2004**, *74* (17), 2185−2197.

(5) Jinadasa, R.; Hu, X.; Vicente, M.; Smith, K. M. Syntheses and Cellular Investigations of 17^3-, 15^2-, and 13^1-Amino Acid Derivatives of Chlorin e_6. *J. Med. Chem.* **2011**, *54* (21), 7464−7476.

(6) Juzeniene, A. Chlorin e6-Based Photosensitizers for Photodynamic Therapy and Photodiagnosis. *Photodiagn. Photodyn. Ther.* **2009**, *6* (2), 94−96.

(7) Ogura, S. i.; Yazaki, K.; Yamaguchi, K.; Kamachi, T.; Okura, I. Localization of Poly-l-lysine-Photosensitizer Conjugate in Nucleus. *J. Controlled Release* **2005**, *103* (1), 1−6.

(8) Usuda, J.; Ichinose, S.; Ishizumi, T.; Hayashi, H.; Ohtani, K.; Maehara, S.; Ono, S.; Honda, H.; Kajiwara, N.; Uchida, O.; et al. Outcome of Photodynamic Therapy Using NPe6 for Bronchogenic Carcinomas in Central Airways > 1.0 cm in Diameter. *Clin. Cancer Res.* **2010**, *16* (7), 2198−2204.

(9) Wang, H.; Jiang, J.; Xiao, J.; Gao, R.; Lin, F.; Liu, X. Porphyrin with Amino Acid Moieties: A Tumor Photosensitizer. *Chem.-Biol. Interact.* **2008**, *172* (2), 154−158.

(10) Serra, V. V.; Andrade, S. M.; Neves, M. G.; Cavaleiro, J. A.; Costa, S. M. J-Aggregate Formation in bis-(4-Carboxyphenyl)-porphyrins in Water: pH and Counterion Dependence. *New J. Chem.* **2010**, *34* (12), 2757−2765.

(11) Choi, Y.; McCarthy, J. R.; Weissleder, R.; Tung, C. H. Conjugation of a Photosensitizer to an Oligoarginine-based Cell-penetrating Peptide Increases the Efficacy of Photodynamic Therapy. *ChemMedChem* **2006**, *1* (4), 458−463.

(12) Saboktakin, M. R.; Tabatabaee, R. M. The Novel Polymeric Systems for Photodynamic Therapy Technique. *Int. J. Biol. Macromol.* **2014**, *65* (0), 398−414.

(13) Master, A. F.; Livingston, M. F.; Sen Gupta, A. Photodynamic Nanomedicine in the Treatment of Solid Tumors: Perspectives and Challenges. *J. Controlled Release* **2013**, *168*, 88−102.

(14) Vermathen, M.; Marzorati, M.; Bigler, P. Self-assembling Properties of Porphyrinic Photosensitizers and their Effect on Membrane Interactions Probed by NMR Spectroscopy. *J. Phys. Chem. B* **2013**, *117*, 6990−7001.

(15) Copley, L.; van der Watt, P.; Wirtz, K. W.; Parker, M. I.; Leaner, V. D. Photolon, a Chlorin e6 Derivative, Triggers ROS Production and Light-Dependent Cell Death via Necrosis. *Int. J. Biochem. Cell Biol.* **2008**, *40* (2), 227−235.

(16) Chin, W. W. L.; Heng, P. W. S.; Bhuvaneswari, R.; Lau, W. K. O.; Olivo, M. The Potential Application of Chlorin e6-Polyvinylpyrrolidone Formulation in Photodynamic Therapy. *Photochem. Photobio. Sci.* **2006**, *5* (11), 1031−1037.

(17) Chin, W. W. L.; Lau, W. K. O.; Bhuvaneswari, R.; Heng, P. W. S.; Olivo, M. Chlorin e6-Polyvinylpyrrolidone as a Fluorescent Marker for Fluorescence Diagnosis of Human Bladder Cancer Implanted on the Chick Chorioallantoic Membrane Model. *Cancer Lett.* **2007**, *245* (1−2), 127−133.

(18) Chin, W. W. L.; Heng, P. W. S.; Thong, P. S. P.; Bhuvaneswari, R.; Hirt, W.; Kuenzel, S.; Soo, K. C.; Olivo, M. Improved Formulation of Photosensitizer Chlorin e6 Polyvinylpyrrolidone for Fluorescence Diagnostic Imaging and Photodynamic Therapy of Human Cancer. *Eur. J. Pharm. Biopharm.* **2008**, *69* (3), 1083−1093.

(19) Ali-Seyed, M.; Bhuvaneswari, R.; Soo, K. C.; Olivo, M. Photolon - Photosensitization Induces Apoptosis via ROS-Mediated Cross-Talk Between Mitochondria and Lysosomes. *Int. J. Oncol.* **2011**, *39* (4), 821−831.

(20) Chin, W. W. L.; Praveen, T.; Heng, P. W. S.; Olivo, M. Effect of Polyvinylpyrrolidone on the Interaction of Chlorin e6 with Plasma Proteins and its Subcellular Localization. *Eur. J. Pharm. Biopharm.* **2010**, *76* (2), 245−252.

(21) Isakau, H. A.; Parkhats, M. V.; Knyukshto, V. N.; Dzhagarov, B. M.; Petrov, E. P.; Petrov, P. T. Toward Understanding the High PDT Efficacy of Chlorin e6-Polyvinylpyrrolidone Formulations: Photophysical and Molecular Aspects of Photosensitizer-Polymer Interaction in vitro. *J. Photochem. Photobiol., B* **2008**, *92* (3), 165−174.

(22) Paul, S.; Selvam, S.; Heng, P. W. S.; Chan, L. W. Elucidation of Monomerization Effect of PVP on Chlorin e6 Aggregates by Spectroscopic, Chemometric, Thermodynamic and Molecular Simulation Studies. *J. Fluoresc.* **2013**, *23* (5), 1065−1076.

(23) Fielding, L. Determination of Association Constants (K_a) from Solution NMR Data. *Tetrahedron* **2000**, *56* (34), 6151−6170.

(24) Thordarson, P. Determining Association Constants from Titration Experiments in Supramolecular Chemistry. *Chem. Soc. Rev.* **2011**, *40* (3), 1305−1323.

(25) Butts, C. P.; Jones, C. R.; Towers, E. C.; Flynn, J. L.; Appleby, L.; Barron, N. J. Interproton Distance Determinations by NOE - Surprising Accuracy and Precision in a Rigid Organic Molecule. *Org. Biomol. Chem.* **2011**, *9* (1), 177−184.

(26) Čunderliková, B.; Gangeskar, L.; Moan, J. Acid-Base Properties of Chlorin e_6: Relation to Cellular Uptake. *J. Photochem. Photobiol., B* **1999**, *53* (1−3), 81−90.

(27) Zhiyentayev, T. M.; Boltaev, U. T.; Solov'eva, A. B.; Aksenova, N. A.; Glagolev, N. N.; Chernjak, A. V.; Melik-Nubarov, N. S. Complexes of Chlorin e6 with Pluronics and Polyvinylpyrrolidone: Structure and Photodynamic Activity in Cell Culture. *Photochem. Photobiol.* **2014**, *90* (1), 171−182.

(28) Jia, Z.; Choi, D. S.; Chokshi, H. Determination of Drug-Polymer Binding Constants by Affinity Capillary Electrophoresis for Aryl Propionic Acid Derivatives and Related Compounds. *J. Pharm. Sci.* **2013**, *102* (3), 960−966.

(29) Radzicka, A.; Wolfenden, R. Comparing the Polarities of the Amino-Acids - Side-Chain Distribution Coefficients Between the Vapor-Phase, Cyclohexane, 1-Octanol, and Neutral Aqueous-Solution. *Biochemistry* **1988**, *27* (5), 1664−1670.

(30) Wolfenden, R. Experimental Measures of Amino Acid Hydrophobicity and the Topology of Transmembrane and Globular Proteins. *J. Gen. Physiol.* **2007**, *129* (5), 357−362.

(31) Avram, L.; Cohen, Y. Diffusion NMR of Molecular Cages and Capsules. *Chem. Soc. Rev.* **2015**, *44* (2), 586−602.

(32) Cameron, K. S.; Fielding, L. NMR Diffusion Spectroscopy as a Measure of Host-Guest Complex Association Constants and as a Probe of Complex Size. *J. Org. Chem.* **2001**, *66* (21), 6891−6895.

(33) Macura, S.; Ernst, R. R. Elucidation of Cross Relaxation in Liquids by Two-Dimensional N.M.R. Spectroscopy (Reprinted from Molecular Physics, vol 41, pg 95−117, 1980). *Mol. Phys.* **2002**, *100* (1), 135−147.

(34) Tsvetkov, V. B.; Solov'eva, A. B.; Melik-Nubarov, N. S. Computer Modeling of the Complexes of Chlorin e6 with Amphiphilic Polymers. *Phys. Chem. Chem. Phys.* **2014**, *16* (22), 10903−10913.

(35) Aksenova, N. A.; Oles, T.; Sarna, T.; Glagolev, N. N.; Chernjak, A. V.; Volkov, V. I.; Kotova, S. L.; Melik-Nubarov, N. S.; Solovieva, A. B. Development of Novel Formulations for Photodynamic Therapy on the Basis of Amphiphilic Polymers and Porphyrin Photosensitizers. Porphyrin-Polymer Complexes in Model Photosensitized Processes. *Laser Phys.* **2012**, *22* (10), 1642−1649.

DOI: 10.1021/acs.jpcb.5b05761
J. Phys. Chem. B 2015, 119, 12117−12128